
Since January 2020 Elsevier has created a COVID-19 resource centre with free information in English and Mandarin on the novel coronavirus COVID-19. The COVID-19 resource centre is hosted on Elsevier Connect, the company's public news and information website.

Vaccine 36 (2018) 3124–3133

Contents lists available at ScienceDirect

Vaccine

journal homepage: www.elsevier.com/locate/vaccine

# High-cell-density cultivations to increase MVA virus production

Daniel Vázquez-Ramírez [a,*], Yvonne Genzel [a], Ingo Jordan [b,1], Volker Sandig [b], Udo Reichl [a,c]

[a] Max Planck Institute for Dynamics of Complex Technical Systems, Sandtorstr. 1, 39106 Magdeburg, Germany
[b] ProBioGen AG, Goethestr. 54, 13086 Berlin, Germany
[c] Chair for Bioprocess Engineering, Otto-von-Guericke-University Magdeburg, Universitätsplatz 2, 39106 Magdeburg, Germany

ARTICLE INFO

*Article history:*
Available online 9 February 2018

*Keywords:*
Viral vaccine production
Process intensification
ATF
Bioreactor
Perfusion
Fed-batch
Scale-down

ABSTRACT

Increasing the yield and the productivity in cell culture-based vaccine manufacturing using high-cell-density (HCD) cultivations faces a number of challenges. For example, medium consumption should be low to obtain a very high concentration of viable host cells in an economical way but must be balanced against the requirement that accumulation of toxic metabolites and limitation of nutrients have to be avoided. HCD cultivations should also be optimized to avoid unwanted induction of apoptosis or autophagy during the early phase of virus infection. To realize the full potential of HCD cultivations, a rational analysis of the cultivation conditions of the appropriate host cell line together with the optimal infection conditions for the chosen viral vaccine strain needs to be performed for each particular manufacturing process.

We here illustrate our strategy for production of the modified vaccinia Ankara (MVA) virus isolate MVA-CR19 in the avian suspension cell line AGE1.CR.pIX at HCD. As a first step we demonstrate that the adjustment of the perfusion rate strictly based on the measured cell concentration and the glucose consumption rate of cells enables optimal growth in a 0.8 L bioreactor equipped with an ATF2 system. Concentrations up to $57 \times 10^6$ cells/mL (before infection) were obtained with a viability exceeding 95%, and a maximum specific cell growth rate of 0.019 $h^{-1}$ (doubling time = 36.5 h). However, not only the cell-specific MVA-CR19 virus yield but also the volumetric productivity was reduced compared to infections at conventional-cell-density (CCD).

To facilitate optimization of the virus propagation phase at HCD, a larger set of feeding strategies was analyzed in small-scale cultivations using shake flasks. Densities up to $63 \times 10^6$ cells/mL were obtained at the end of the cell growth phase applying a discontinuous perfusion mode (semi-perfusion) with the same cell-specific perfusion rate as in the bioreactor (0.060 nL/(cell d)). At this cell concentration, a medium exchange at time of infection was required to obtain expected virus yields during the first 24 h after infection. Applying an additional fed-batch feeding strategy during the whole virus replication phase resulted in a faster virus titer increase during the first 36 h after infection. In contrast, a semi-continuous virus harvest scheme improved virus accumulation and recovery at a rather later stage of infection. Overall, a combination of both fed-batch and medium exchange strategies resulted in similar cell-specific virus yields as those obtained for CCD processes but 10-fold higher MVA-CR19 titers, and four times higher volumetric productivity.



## 1. Introduction

Modern recombinant vector vaccines combine the advantages of an attenuated or even host-restricted infection with a highly immunogenic expression of an antigen of choice. Especially promising vectors are highly attenuated poxviruses, including modified vaccinia virus Ankara (MVA) [1]. MVA has been attenuated by repeated passaging in chicken fibroblast cultures [2], and its properties as potential human vector vaccine have been well characterized [1,3–11]. Various MVA recombinants that express different viral heterologous antigens have been generated and extensively tested in pre-clinical and clinical trials as candidate vaccine against diseases such as AIDS, influenza, severe acute respiratory syndrome (SARS) and human respiratory syncytial virus (RSV) infection [7,9–11]. The use of MVA as a vector-based vaccine, however, is predicted to require highly concentrated doses of about $10^8$ infectious units (IU) per mL [1,6], preferably produced in media free of animal-derived components.

* Corresponding author.
*E-mail address:* vazquez_ramirez@mpi-magdeburg.mpg.de (D. Vázquez-Ramírez).
[1] Current address: CureVac AG, Paul-Ehrlich-Str. 15, 72076 Tübingen, Germany.

https://doi.org/10.1016/j.vaccine.2017.10.112
0264-410X/

MVA (similar to other viruses such as influenza A virus or yellow fever virus) is being produced in material obtained from embryonated chicken eggs or primary chicken embryo fibroblasts (CEF) [8]. However, the use of primary animal-derived material that is continuously fed into vaccine production processes is not an optimal scenario. To overcome this problem, two fully permissive avian suspension cell lines, AGE1.CR (in the following CR) and AGE1.CR.pIX (in the following CR.pIX) were developed [12] and adapted to proliferation in a chemically defined medium to enable the establishment of robust high-yield production processes [13–15]. Because MVA spreads preferably via cell-to-cell contact a culture format was developed where cell agglomerates of infected and non-infected cells are being induced for production of vaccine preparations. A MVA strain (MVA-CR19) was recently obtained with this system that propagates also in non-agglomerated CR.pIX suspension cells [16]. With this new isolate that represents a different genotype of MVA, titers in the order of $10^8$ IU/mL can be obtained at conventional-cell-densities (CCD) of about $2.0 \times 10^6$ cells/mL. As a higher fraction of MVA-CR19 is released into the supernatant, harvest of infectious units does not require whole-cell lysates anymore, facilitating the subsequent downstream processing [16].

To further increase virus titers, high-cell-density (HCD) processes can be established [17]. While virus propagation in HCD often results either in a decrease in cell-specific yields [18,19] – the so-called "cell-density effect" [20,21] – or in low volumetric productivity [22], there are reports on positive effects on virus titers and cell-specific yields if certain medium feeding/exchange strategies prior to or during virus propagation are being applied. The described strategies can involve medium recirculation, medium perfusion, and periodic virus harvesting [17]. However, in most of these approaches adherent cell lines were used with limited options for scale-up and process intensification. A few authors described the use of suspension cells at $10^7$ cells/mL [22–26], but without addressing details of optimization.

Here, an analysis regarding the effect of various medium feeding strategies before and after infection on the yields for production of MVA-CR19 in suspension CR.pIX cells at HCD ($50–63 \times 10^6$ cells/mL) is presented. Cultivations were performed in perfusion bioreactor and shake flasks as a small-scale model. We demonstrate that by applying optimized feeding strategies at HCD, similar cell-specific virus yields can be obtained while maximum virus titers as well as volumetric productivity can be increased significantly compared to CCD cultivations.

## 2. Materials and methods

### 2.1. Cells and medium

Suspension CR.pIX cells [12] were cultivated in chemically defined CD-U3 medium (Biochrom GmbH) with a glucose concentration of 33–40 mM, supplemented with glutamine, alanine (both 2 mM final concentration, Sigma), and recombinant insulin-like growth factor (LONG-R3IGF, 10 ng/mL final concentration, Sigma). Cells were passaged twice a week at a seed concentration of $0.8 \times 10^6$ cells/mL.

### 2.2. Cultivation in bioreactor

CR.pIX cells were cultivated in a lab-scale bioreactor (BIOSTAT®B plus, Sartorius AG) with a working volume of 0.8 L. The bioreactor was inoculated at $0.8 \times 10^6$ cells/mL with pre-cultures expanded in 250 mL shake flasks and operated at 37 °C, pH 7.2, and a stirring speed of 120–160 rpm. Dissolved oxygen concentration (DO) was controlled at 40% by pulsed aeration with pure oxygen through a 20 $\mu$m pore size micro-sparger to a maximum of 0.048 vvm, representing a volumetric oxygen transfer coefficient ($k_La$) of 10.85 $h^{-1}$ at 142 rpm. Cells were initially cultivated in batch until a glucose concentration of 14–17 mM (60–72 h after inoculation) was reached. At that point, perfusion was started using an ATF2 perfusion system controlled by the C24U–V2.0 controller from Refine Technology and a polysulfone 500 kDa hollow fiber cartridge (UFP-500-E-4X2MA, GE Healthcare). Cell suspension was pumped through the hollow fiber with a recirculation rate of 1.0 L/min and fed with defined perfusion rates to achieve a minimum concentration of $50 \times 10^6$ cells/mL.

Feeding was based on a constant cell-specific perfusion rate (CSPR) [27] taking into account the steady state mass balance for substrates as described by Kompala and Ozturk [28] with glucose as the major energy source for CR.pIX cells [29] as:

$$CSPR = D/x = q_{g/x}/(C_{gM} - C_{gR}) \quad (1)$$

with the dilution rate (D, $h^{-1}$), the viable cell concentration (x, cells/mL), a cell-specific glucose consumption rate ($q_{g/x}$) of $8.54 \times 10^{-11}$ mmol/(cell h) (based on previous data, not shown), a glucose concentration in CD-U3 medium ($C_{gM}$) of 33–40 mmol/mL, and a glucose concentration in the bioreactor ($C_{gR}$) of 6 mmol/mL.

As D is the ratio between the perfusion rate Q (mL/h) and the reactor's working volume $V_w$ (mL), the perfusion rate Q as a function of time can be expressed as:

$$Q = x_i\, e^{\mu t}\, V_w\, CSPR \quad (2)$$

Q was adjusted manually according to the initial cell concentration $x_i$ to cover the increasing nutrient demand (i.e. glucose) until the next sampling time point (for simplicity reason either 12 or 24 h). Therefore, the cascade control of the BIOSTAT®B plus module was used. For all calculations a constant cell-specific growth rate $\mu$ = 0.026 $h^{-1}$ was considered.

Three hours before infection, the perfusion rate was set to 2.5 times its calculated value to achieve a total medium exchange of 0.85 reactor volumes to further reduce the risk of nutrient limitation, and to dilute unwanted by-products that could negatively affect virus propagation. After infection, the perfusion rate was adjusted to the calculated values, applying the same $\mu$ as for the cell growth phase. From 36 hours post infection (hpi) a specific cell death rate of 0.028 $h^{-1}$ was taken into account to compensate for increasing cell losses due to progress of infection (based on previous data, not shown).

### 2.3. Shake flask cultivations

Small-scale cultivations were carried out in shake flasks with baffles (#215-2273, 125 mL (50 mL $V_w$) or #215-2277, 250 mL (110 mL $V_w$), VWR International, LLC) at 37 °C, 5% $CO_2$ and 185 rpm agitation speed in a Multitron incubation shaker (Infors AG) with 5 cm orbit. For experiments at CCD, shake flasks were inoculated to $0.8–0.9 \times 10^6$ cells/mL and cultivated for 72 h to reach about $4.0 \times 10^6$ cells/mL before infection. For experiments at HCD, the same inoculation procedure was performed and cells were cultivated in batch for 72 h before starting semi-perfusion.

Semi-perfusion was carried out by exchanging periodically enough medium to cover the glucose demand between two sampling time points. Assuming that the medium exchange volume ($V_E$) should equal the amount of medium exchanged in a continuous perfusion process for the same time period, $V_E$ can be derived solving Eq. (2) for $d(V_E) / dt = x_i\, e^{\mu t}\, V_w\, CSPR$ to obtain:

$$V_E = \mu^{-1}\, x_i\, (e^{\mu\, \Delta t} - 1)\, V_w CSPR \quad (3)$$

Depending on the viable cell concentration $x_i$ at the initial sampling time point, $V_E$ (typically less than 60% of $V_w$) was calculated considering a CSPR of 0.060 nL/(cell d) (based on the perfusion culture performed in the bioreactor) and a $\Delta t$ of 8–24 h.

The calculated volume was removed from the cell culture and centrifuged at 200*g* for 5 min. The supernatant was discarded, the cell pellet re-suspended in the same volume of fresh medium and returned to the shake flask. Fluctuations in the concentration of medium components were avoided by regularly adjusting the frequency of medium exchange (maximum 60% $V_w$). In order to assure a homogeneous cell population at time of infection (TOI), cells were expanded in parallel in 250 mL shake flasks (110 mL $V_w$). Additionally, at each time point of medium exchange, cells from all shake flasks were pooled, sampled and the exchange volume calculated based on the pooled cell concentration. When a minimum target concentration of $50 \times 10^6$ cells/mL was achieved, cells were distributed to 125 mL shake flasks (50 mL $V_w$) and infected accordingly.

At TOI, for infections comprising a total or a partial medium exchange, the corresponding volume of cell broth was centrifuged at 200*g* for 5 min and the cell pellet re-suspended in the respective volume of fresh medium containing the virus. When required, pH and DO were monitored online using an SFR® system (PreSens).

### 2.4. Virus

A seed virus bank of the MVA-CR19 isolate ($4.5 \times 10^8$ virions/mL) propagated in CR.pIX cells was prepared as described before [16]. Before infection, seed virus aliquots were treated for 1 min in a sonication water bath to break up virus aggregates. All cultivations were infected at an MOI (multiplicity of infection) of 0.05 virions/cell. Infections at CCD ($4.0 \times 10^6$ cells/mL) were performed as described by Lohr (2014) [30], diluting the cell culture 1:2 with fresh CD-U3 medium containing the defined amount of virus. Hence a final concentration of $2.0 \times 10^6$ cells/mL was obtained after infection. For infections in HCD, the seed virus was diluted in fresh medium and added when a total or partial medium exchange at TOI was performed. For infection in bioreactors or when no medium exchange was performed, the virus was diluted in fresh medium with a volume equal to 5–6% of the $V_w$, and added to the cell culture.

For quantification of the concentration of infectious virus particles (here lysate), infected cells were treated with three freeze/thaw cycles (−80 °C/RT) and treated for 1 min in a sonication water bath (45 kHz) prior to centrifugation at 1500*g*, 10 min, RT, to discard cellular debris. For the quantification of virus released by host cells (here supernatant), samples were centrifuged at 200*g*, 5 min, RT, supernatant was retrieved and treated also with three freeze/thaw cycles before storage [16]. All virus samples were stored in aliquots of 0.5–1 mL at −80 °C. Virus quantification was performed by $TCID_{50}$ as described previously [12].

The cell-specific virus yield ($Y_{v/cell}$, virions/cell) was calculated based on the total number of infectious virus particles ($vir_T$) and the total number of cells produced ($cell_T$). The latter differed from the number of cells at TOI since cell growth was typically observed up to 36–48 hpi.

Similarly, the volumetric productivity ($P_V$, virions/(L d)) was calculated considering $vir_T$, the total spent medium during cell growth and virus replication phase ($V_T$, L), and the total process time ($t_T$, d), using Eq. (4):

$$P_V = vir_T / (V_T t_T) \quad (4)$$

In order to analyze the productivity at different time points over the virus infection phase, an "apparent" cell-specific virus yield ($Y_{v/cell\ app}$, virions/cell) was calculated considering the number of virus particles produced until that time point ($vir_{acc}$) and the number of cells infected at 0 hpi ($cell_{0hpi}$), according to Eq. (5):

$$Y_{v/cell\ app} = vir_{acc}/cell_{0hpi} \quad (5)$$

### 2.5. Determination of cell and metabolite concentrations

Samples from bioreactor cultures were taken with a syringe (6–8 mL) through a Luer-Lock-septum in 12–24 h intervals and stored at −80 °C until analysis. For determination of glucose and lactate concentrations, a validated assay using a Bioprofile 100 Plus (Nova Biomedical) was used as described previously [15]. Cell concentrations were determined with the cell counter ViCell-XR (Beckman Coulter) with a validated relative standard deviation of 2.48% [30].

### 2.6. Flow cytometry

The percentage of infected cells at different time points post infection was determined with flow cytometry. A total amount of $1 \times 10^6$ infected cells were fixed using 1–2% paraformaldehyde for 30 min at 4 °C. Fixed cells were washed once with phosphate buffered saline (PBS) and permeabilized with 0.5% Tween 20 in PBS at 4 °C for 5 min. The cells were immuno-stained with 1:100 diluted FITC-conjugated polyclonal anti-vaccinia antibody (1952402357, quartett GmbH) in staining buffer containing PBS plus 1% foetal calf serum (FCS) for 1–2 h in dark at RT. Using the ImageStream X Mark II (Amnis, EMD Millipore) 10,000 single cells per sample (debris and cell doublets were excluded) were analyzed at a wavelength of 488 nm at 5 mV intensity. Data analysis was performed using the IDEAS and FlowJo software.

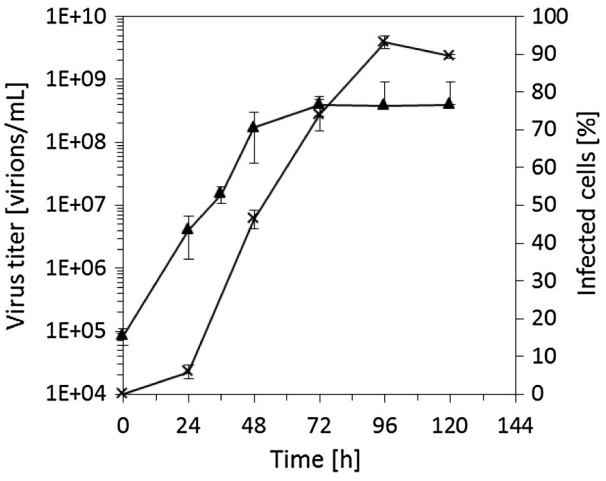


**Fig. 1.** MVA-CR19 propagation in CR.pIX cells infected at CCD ($2.0 \times 10^6$ cells/mL) in shake flasks. Virus titer (▲), percentage of infected cells (×). Mean and standard deviation of three independent cultivations.

## 3. Results and discussion

### 3.1. Propagation of MVA-CR19 at CCD

As a reference, infections using CR.pIX cells at CCD were carried out in 50 mL ($V_w$) shake flasks. For all CCD infections in shake flasks, maximum titers of $4.0 \times 10^8$ virions/mL were obtained at about 72 hpi (Fig. 1). This was about 24 h later compared to Jordan et al. [13] who used the same virus isolate, cell line and infection strategy. Despite this difference in virus replication dynamics, set of experiments performed in this study (Table 1, CS19b) showed similar virus titers, cell-specific yields and volumetric productivities as reported previously for shake flasks (Table 1, CSwt, CS19a)

[16,30] and a bioreactor (Table 1, CBwt) [15,30]. Thus, the results obtained were considered as representative for CCD infections.

### 3.2. Propagation of MVA-CR19 in perfusion bioreactor at HCD

Previous experiments using an ATF2 system for the cultivation of CR cells showed the suitability of hollow fiber-based perfusion bioreactors for the production of the influenza virus A/PR/8/34 (H1N1) at HCD [22]. For CR cells a specific oxygen uptake rate of $3.1 \times 10^{-11}$ mmol/(cell h) was determined previously [22]. Assuming a similar rate for CR.pIX cells, a $k_La$ of 2.5 $h^{-1}$ would be required to achieve about $50 \times 10^6$ cells/mL. Accordingly, with operation conditions matching those determined previously for the same bioreactor ($k_La$ = 10.9 $h^{-1}$) [22], an oxygen limitation is not to be expected.

For a concentration targeting $50 \times 10^6$ cells/mL in the perfusion bioreactor, the medium feeding regime described above (see Materials and Methods) led to a constant cell specific growth rate of 0.019 $h^{-1}$ (doubling time, $t_2$ = 36.5 h), except for a short overfeeding (−50 to −36 h) due to a failure in the control of the feeding pump (Fig. 2A and B). To correct the failure, medium addition was stopped for 2 h and medium removed through the hollow fiber to recover the original $V_w$ of 0.8 L. Perfusion was then re-started using the initial regime and $57 \times 10^6$ cells/mL at 95% viability were finally obtained 247 h after inoculation (Fig. 2A). As expected, this perfusion control led to a very stable CSPR of 0.043–0.066 nL/(cell d) demonstrating the robustness of the feeding strategy chosen. Also, medium utilization was considerably reduced to 8.8 reactor volumes ($V_R$) compared to the almost 32 $V_R$ reported previously for CR cells, where $50 \times 10^6$ cells/mL at a similar specific growth rate of 0.020 $h^{-1}$ ($t_2$ = 34) were obtained [22].

The extensive medium exchange during the last 3 h before infection resulted in an increase in the glucose concentration from 3.72 to 11.0 mM. Despite the adjustment of the perfusion rate at an average CSPR of 0.057 nL/(cell d) after infection, the glucose concentration showed a considerable drop from 11.0 to 8.49 mM during the first 12 hpi. In order to prevent a glucose limitation during the early stage of virus replication, the CSPR was increased by 50% from 12 to 36 hpi (Fig. 2B). Afterwards, the perfusion rate was re-adjusted to the theoretical glucose consumption rate.

Given that the initial titer of $3.16 \times 10^6$ virions/mL corresponds actually to a virus concentration that is expected at an MOI of 0.05, loss of the 350 × 270 nm size virions through the 500 kDa ATF membrane is negligible. Additionally, the absence of any active virus in the permeate line (data not shown) along the whole process indicated that all viral particles were indeed retained within the "reaction volume".

With a maximum virus titer of $3.2 \times 10^9$ virions/mL at 72 hpi (Fig. 2B and C), almost a 10-fold increase in the virus titer compared to reference infections at CCD in shake flasks ($4.0 \times 10^8$ virions/mL) was achieved at the same time point post infection (Fig. 1). Overall, a cell-specific yield of 38 virions/cell was obtained (Table 1, HB19) which was 70% lower than for the reference infections at CCD in shake flasks (Table 1, CS19b), and other reported values (Table 1, CS19a, CSwt). Interestingly, in this HCD cultivation, the concentration of viable cells increased significantly after infection (Fig. 2A). In addition, the percentage of infected cells was very low during the first 36 hpi (Fig. 2C). This suggests a delay in the virus uptake and onset of intracellular virus replication. Given the total amount of medium employed for biomass expansion and during virus propagation, the volumetric productivity was also lower compared to the CCD experiments (Table 1, HB19). Taken together, two key factors seemed to be important for further improvement of HCD cultivations:

a. An optimization of infection conditions to achieve fast virus replication after the addition of the seed virus
b. A minimization of medium utilization over the entire virus propagation phase without compromising final virus titers

In order to address these two targets, several feeding strategies were assessed during the virus replication phase in small-scale shake flasks.

### 3.3. Scale-down and optimization of virus yields in semi-perfusion culture in shake flasks

#### 3.3.1. Criteria for scale-down to shake flasks

Conditions for batch cultivation of CR.pIX cells in baffled shake flasks were previously optimized [31], and concentrations up to $10 \times 10^6$ cells/mL with 95% of viability have been routinely obtained (data not shown). However, whether these conditions, especially the shaking frequency (185 rpm), could fulfill oxygen transfer requirements to achieve cell concentrations up to $50 \times 10^6$ cells/mL was not clear. Also, the suitability of a manual medium exchange by centrifugation (semi-perfusion) to mimic perfusion in shake flasks had to be demonstrated.

Hence, the $k_La$ for the described cultivation conditions (37 °C, 185 rpm shaking frequency) was estimated based on an empirical correlation described for shake flasks with same geometrical configuration by Schiefelbein et al. [32]. For the described cultivation conditions, a $k_La$ of 90.4 and 128 $h^{-1}$ should be expected for 125 (50 mL $V_w$) and 250 mL (110 mL $V_w$) shake flasks, respectively. These values are about 10 times higher than the reported $k_La$ of 10.9 $h^{-1}$ for the perfusion bioreactor described above.

Subsequently, the scale-down to 110 mL ($V_w$) shake flasks was analyzed considering the specific cell growth rate, glucose and lactate concentrations, DO and pH as key parameters. Applying a constant CSPR of 0.060 nL/(cell d), cell concentrations above $45 \times 10^6$ cells/mL (Fig. 3A) and a specific growth rate of 0.018 $h^{-1}$ were achieved. Constant medium renewal allowed maintain-

**Table 1**
MVA production in CR.pIX suspension cells for conventional and high-cell-density cultures.

| ID[a] | Working volume [mL] | Harvest titer [virions/mL] | $t_T$ [d][b] | Max. cells [$\times 10^6$/mL] | $Y_{v/cell}$ [virions/cell][c] | $P_V$ [virions/(L × d)][d] |
|---|---|---|---|---|---|---|
| CSwt[e] [27] | 50 | $2.7 \times 10^8$ | 5.0 | 2.7 | $1.0 \times 10^2$ | $5.4 \times 10^{10}$ |
| CBwt[f] [15,27] | 1000 | $1.0 \times 10^8$ | 5.0 | 2.0 | $0.50 \times 10^2$ | $2.0 \times 10^{10}$ |
| CS19a[g] [16] | 50 | $3.0 \times 10^8$ | 5.0 | 2.0 | $1.5 \times 10^2$ | $6.0 \times 10^{10}$ |
| CS19b[g] | 50 | $3.9 \times 10^8$ | 6.0 | 3.0 | $1.3 \times 10^2$ | $6.6 \times 10^{10}$ |
| HB19[f] | 800 | $3.2 \times 10^9$ | 13 | 83 | $0.38 \times 10^2$ | $1.0 \times 10^{10}$ |

[a] C: conventional-cell-density, H: high-cell-density, S: shake flask, B: bioreactor, wt: MVA-wt, 19: MVA-CR19.
[b] Total time from cell inoculation to maximum titer.
[c] Cell-specific virus yield.
[d] Volumetric productivity.
[e] Average of four independent cultivations.
[f] Single bioreactor cultivations.
[g] Average of three independent cultivations.

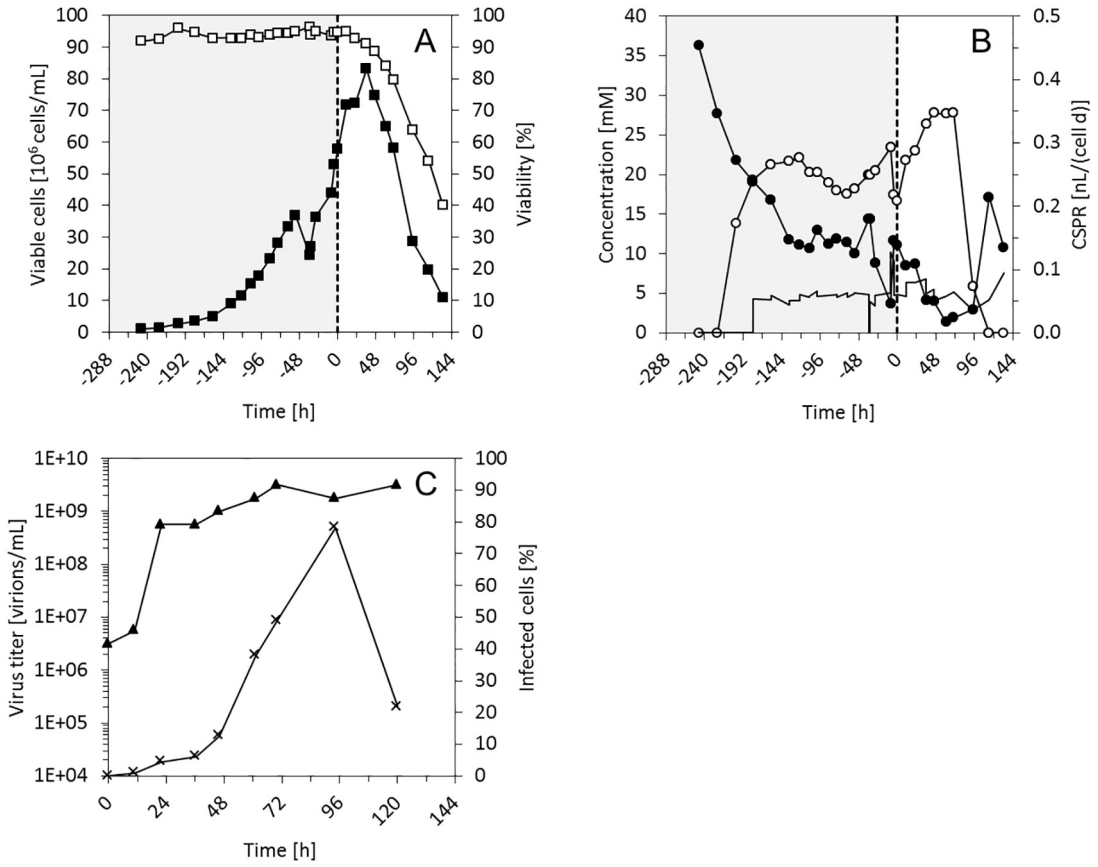


**Fig. 2.** MVA-CR19 propagation in CR.pIX cells infected at HCD ($57 \times 10^6$ cells/mL) in a perfusion bioreactor. A: viable cell concentration (■) and viability (□), B: glucose (●) and lactate (○) concentrations, cell-specific perfusion rate (CSPR) (—); C: virus titer (lysate) (▲), and percentage of infected cells (×). Cell growth phase (shaded area), virus propagation phase (white area).

ing the glucose and lactate concentrations at similar levels as in the HCD bioreactor cultivation (Fig. 3B). In addition, the pH values were in a range of 7.2 ± 0.2 (Fig. 3C), which corresponded to the set-point of bioreactor cultivations. As expected, the DO was maintained at very high levels (>85%, Fig. 3C). Therefore oxygen supply was not considered critical for the HCD cultivations described below.

### 3.3.2. Effect of medium exchanges at time of infection on virus yields

Following the characterization of general growth properties of CR.pIX cells at HCD, the effect of a medium exchange at TOI on virus yields was analyzed. Without medium exchange at TOI, a maximum virus titer of $1.0 \times 10^8$ virions/mL was obtained at 35 hpi (Fig. 4B), despite the subsequent addition of a 10-fold glucose-concentrated CD-U3 medium (0, 22 and 50 hpi) in fed-batch (FB) to avoid energy depletion. This led to a very low cell-specific yield of 2.3 virions/cell and a volumetric productivity of $2.4 \times 10^8$ virions/(L d) (Table 2), which was about one log lower compared to the HCD cultivation in the bioreactor (Table 1). Compared to infections at CCD, the difference was even larger (Table 1). However, MVA-CR19 production considerably improved with a single 50% medium exchange at TOI followed by the addition of concentrated medium only at 21 hpi, when glucose was depleted. Despite a short-term glucose limitation, no negative effect in later virus propagation was observed and maximum virus titers of $3.2 \times 10^9$ virions/mL were obtained at about 72 hpi in both the lysate and the supernatant (Fig. 4D). This demonstrated that 100% of the produced viruses can be harvested from supernatant at 72 hpi with no need of a cell-disrupting operation (e.g. freeze/thaw), as observed previously in CCD infections. With a cell-specific yield of 62 virions/cell and a volumetric productivity of $6.0 \times 10^{10}$ virions/(L d) (Table 2), the results achieved are in the same range as for the HCD perfusion culture performed in the bioreactor (Table 1). This suggested that the medium exchange at TOI rather than the exclusive glucose supply in FB with concentrated medium is required to boost MVA-CR19 virus propagation (especially from 0 to 24 hpi, Fig. 4B and D). Also, it has been reported that glutamine plays a minor role in energy supply for CR.pIX cells and that its absence might not influence the propagation of MVA in this cell line [29]. Therefore, the positive effect of a medium exchange at TOI on virus propagation might be also due to the dilution of inhibitory metabolites or signaling molecules rather than just a better supply of substrates.

### 3.3.3. Effect of the substrate feeding strategy on virus yields

In a final step, the combination of a medium exchange at TOI with various feeding strategies, using CD-U3 medium, was investigated. The cellular material for the HCD cultures was generated from two 110 mL ($V_w$) batch cultures (in two 250 mL shake flasks). In order to shorten the cell growth phase, the cells were inoculated at $1.1 \times 10^6$ cells/mL and semi-perfusion was performed with a strict control of the time and the frequency of the medium exchange. Cell concentrations increased without any noticeable lag phase with a maximum specific growth rate of 0.023 $h^{-1}$ ($t_2$ = 30 h), similar to other batch cultivations [30]. The culture was split into three 125 mL shake flasks after $63 \times 10^6$ cells/mL were obtained to investigate the infection strategies described below.

To further reduce the risk of glucose limitation observed at 24 hpi with a 50% of medium exchange at TOI, a 100% medium

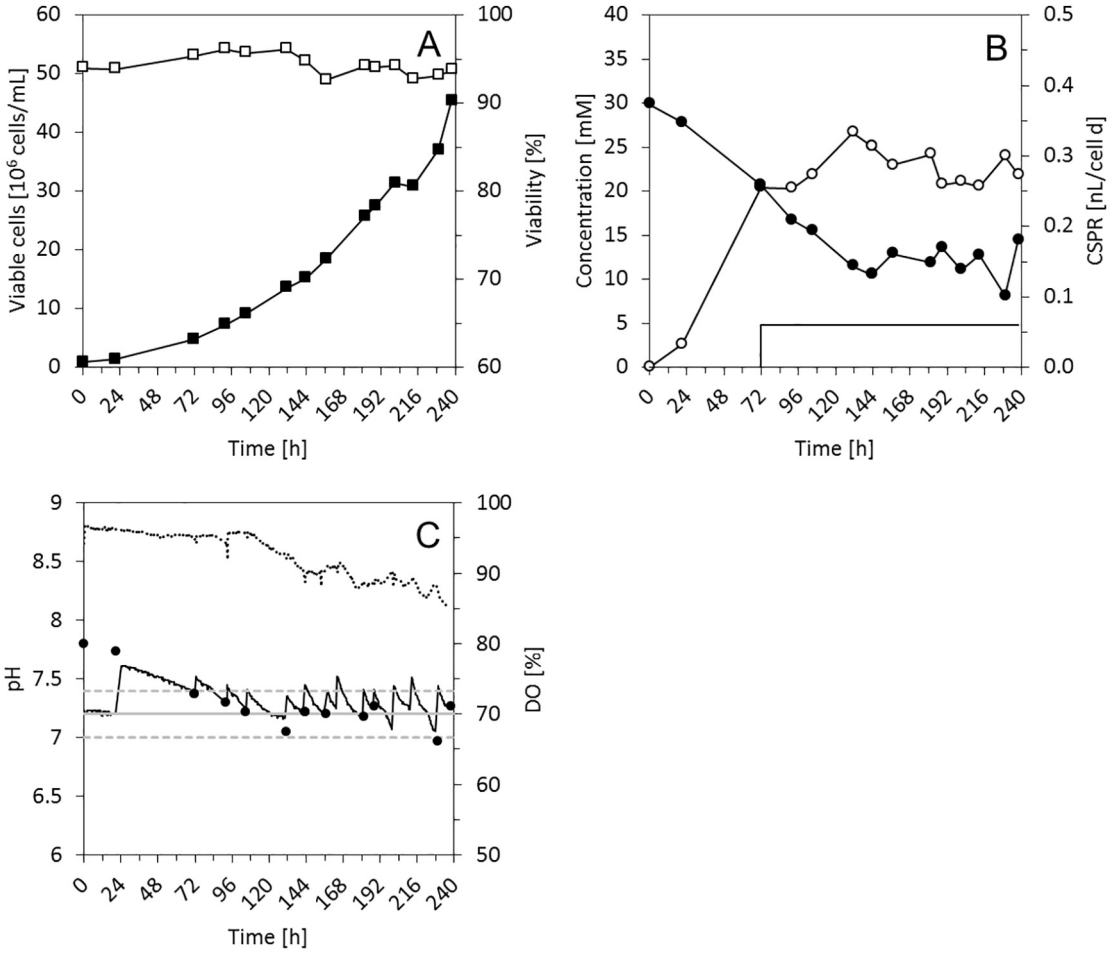


**Fig. 3.** Growth of CR.pIX cells at HCD in 250 mL shake flasks (110 mL $V_w$). A: viable cell concentration (■) and viability (□), B: glucose (●) and lactate (○) concentrations, cell-specific perfusion rate (CSPR) (—); C: online DO (•••), online (—) and offline pH (●). Continuous gray line: optimal pH, dashed gray lines: ±0.2 pH units.

exchange at TOI followed by three alternative feeding strategies was analyzed:

I. Fed-batch (FB): a similar strategy to the volume-expanded fed-batch (VEF-batch) protocol used for the production of *Parapoxvirus ovis* in bovine kidney cells previously reported by Pohlscheidt et al. [33], was carried out. A medium volume equal to the working volume at TOI (i.e. 20 mL) was added at time points 12, 24, 36 and 72 hpi (Fig. 5D). At 36 hpi, a working volume of 80 mL was reached (which is above the maximum working volume in the 125 mL shake flasks) and the cell suspension was transferred to a 250 mL shake flask to continue the experiment.
II. Daily medium exchange (DME): 90% of the culture supernatant was exchanged every 24 h. This was achieved by centrifugation of the complete volume of the shake flask at 200*g*, 10 min, followed by harvest of 90% of the supernatant, and addition of fresh medium. $V_w$ at TOI: 50 mL.
III. Combination of fed-batch and daily medium exchange (F+D): medium was added in the fed-batch mode (see I.) at 12 and 24 hpi. 90% of culture supernatant was exchanged at 36, 72 and 96 hpi. As before, the supernatants were collected as product harvest. $V_w$ at TOI: 20 mL.

Even a 100% medium exchange at TOI and 24 hpi could not completely prevent temporary depletions of glucose within the DME strategy (Fig. 5E, 24 and 48 hpi). Similarly glucose limitations were observed at 24 and 72 hpi for the F+D (Fig. 5F) strategy. However, these short-term limitations did not compromise virus propagation: with virus titers higher than $1.0 \times 10^8$ virions/mL within the first 24 hpi (Fig. 5G–I) all experiments performed better than those with a 50% medium exchange (Fig. 4D). Interestingly, the increase in volume for FB (Fig. 5D) and F+D (Fig. 5F) during the first 24 hpi did not result in a noticeable reduction of virus titers compared to the DME strategy (Fig. 5E). This positive effect of volume changes on virus titers, despite their expected reduction due to product dilution, was also documented previously for the volume-expanded fed-batch strategy [33]. At 36 hpi, the DME strategy showed a slight decrease in virus accumulation compared to both other strategies. This is possibly due to the removal of infectious particles (harvest of 90% supernatant) and a glucose limitation at 24 hpi. This contrasted with the FB and F+D strategies, where titers above $1.0 \times 10^9$ virions/mL were reached at 36 hpi. Nevertheless, a daily exchange of medium (DME, F+D strategy) extended the virus production phase, and allowed to achieve virus titers up to $1.0 \times 10^{10}$ virions/mL at 72 hpi. In contrast, the maximum titer was only $3.7 \times 10^9$ virions/mL for the FB at the same time point (Fig. 5G–I). Product harvests (supernatant) obtained for the DME and F+D strategies showed consistently very similar virus titers to the lysates (except for harvests at 36 hpi in F+D) and even same titers at 72 hpi. Titers in this range were also obtained by Jordan et al. [16]. Accordingly, MVA-CR19 propagation in the CR.pIX cells does not require any disruption steps of the host cells to achieve very high product titers in HCD cultivations.

As another comparison between the different feeding strategies, the increase in the $Y_{v/cell\ app}$, in which only cells infected at 0 hpi

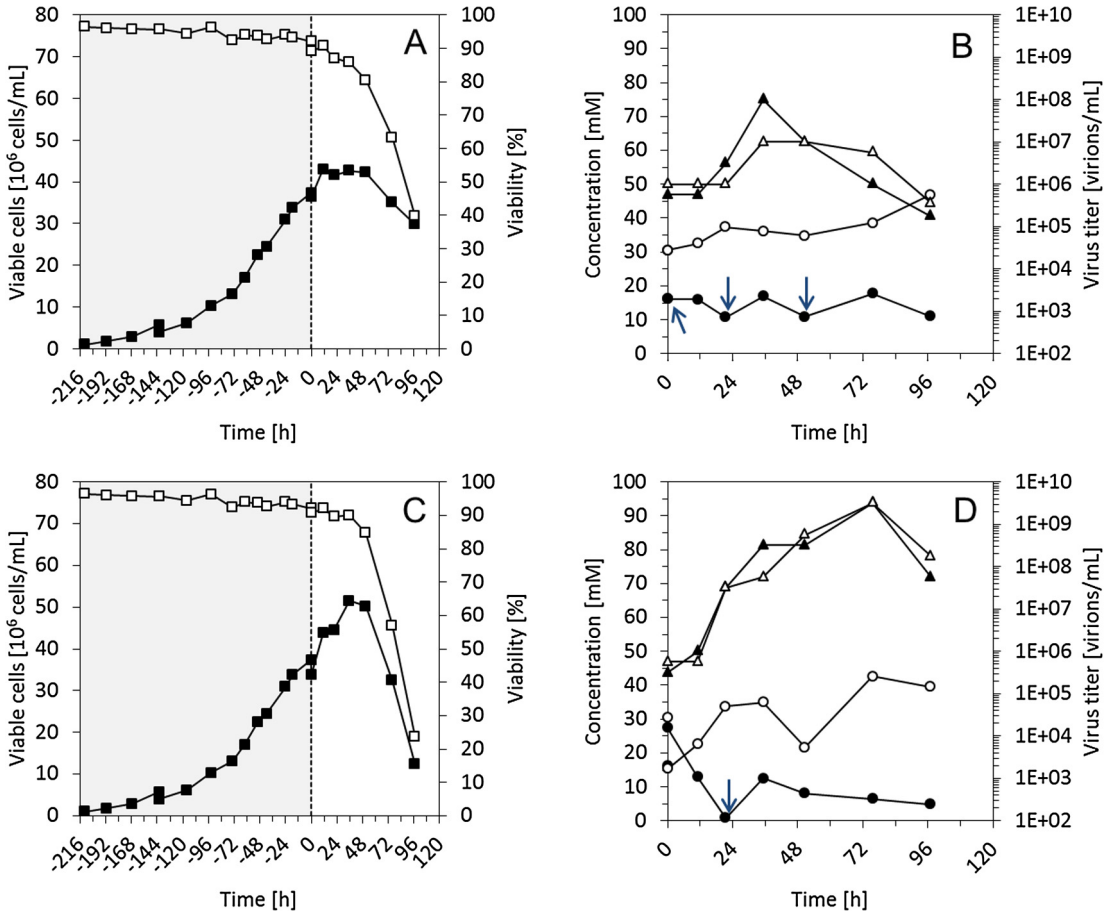


**Fig. 4.** MVA-CR19 propagation in CR.pIX cells infected at HCD ($37 \times 10^6$ cells/mL) in 250 mL shake flasks (110 mL $V_w$). Viable cell concentration (■) and viability (□) without medium exchange (A) and 50% medium exchange (C) at time of infection. Glucose (●) and lactate (○) concentrations and virus titer in lysate (▲) and supernatant (△), without medium exchange (B) and 50% medium exchange (D). Cell growth phase (shaded area), virus propagation phase (white area), time-points of glucose-concentrated medium addition (arrows).

**Table 2**
MVA-CR19 production in CR.pIX suspension cells in shake flasks at high-cell-density without and with 50% medium exchange at time of infection.

| Medium exchange | Harvest titer [virions/mL] | $Y_{v/cell}$ [virions/cell] | $P_V$ [virions/(L × d)] |
|---|---|---|---|
| 0% | $1.0 \times 10^8$ | 2.3 | $2.4 \times 10^8$ |
| 50% | $3.2 \times 10^9$ | 62 | $6.0 \times 10^{10}$ |

are taken into account, and in $P_V$ over the infection time are shown in Fig. 6A and B, respectively. Both FB-based strategies are superior to the DME strategy regarding onset of virus release and maximum $Y_{v/cell\ app}$. Furthermore, the maximum $Y_{v/cell\ app}$ of the F+D strategy exceeds the yield of both other approaches by a factor of two or three. Regarding the $P_V$, the difference between the feeding strategies is smaller. As expected, the difference becomes less evident for the overall cell-specific yield (Table 3), which takes into account cells produced even after TOI. However, FB-based strategies (FB and F+D) showed up to two times higher maximum cell-specific yields compared to DME (Table 3), which indicates an optimal balance between the maintenance of healthy cells and the progress of virus replication. This observation is also supported by the higher percentage of infected cells obtained for the FB and F+D strategies (Fig. 5G–I). In summary, all strategies led to higher cell-specific yields compared to the typical process at CCD.

Since cells of all analyzed strategies originated from one single HCD-cultivation, for the calculation of volumetric productivities, the corresponding medium utilization of each strategy during the cell growth phase was calculated based on their $V_w$ at TOI. This way, medium utilization until TOI was considered 60% lower for FB and F+D strategies ($V_w$ = 20 mL) compared to the DME ($V_w$ = 50 mL). Accordingly, the F+D strategy provided the best volumetric productivity, since it provided the lowest medium consumption during the cell expansion phase and produced the highest amount of virus particles (Table 3). Overall, the F+D strategy optimally combined a low medium consumption with high yields. Another positive feature of substrate feeding in a fed-batch mode is that no virus is lost at early stages of infection, which helps to reach a higher fraction of infected cells and high titers at about 36 hpi (Fig. 5G–I) without reaching limiting glucose concentrations. At that time point, a first harvest should also be considered to collect a highly concentrated supernatant and to avoid the accumulation by-products with a negative impact on virus replication (compare time course of virus titers in Fig. 5G and I). Furthermore, a transfer of the cell suspension to a new vessel was not required for the F+D strategy, which represents an advantage against the FB and the reported VEF-batch [33] regarding the operation of large bioreactors.

In accordance to the more than 10-fold increase in cell concentrations, all strategies resulted in product titers 10 times higher than the titers typically obtained at CCD. This was also observed regarding the slight increase in cell-specific yields. Even more significant was the considerable increase in volumetric productivity of up to four times in the case of the F+D strategy (Table 3).

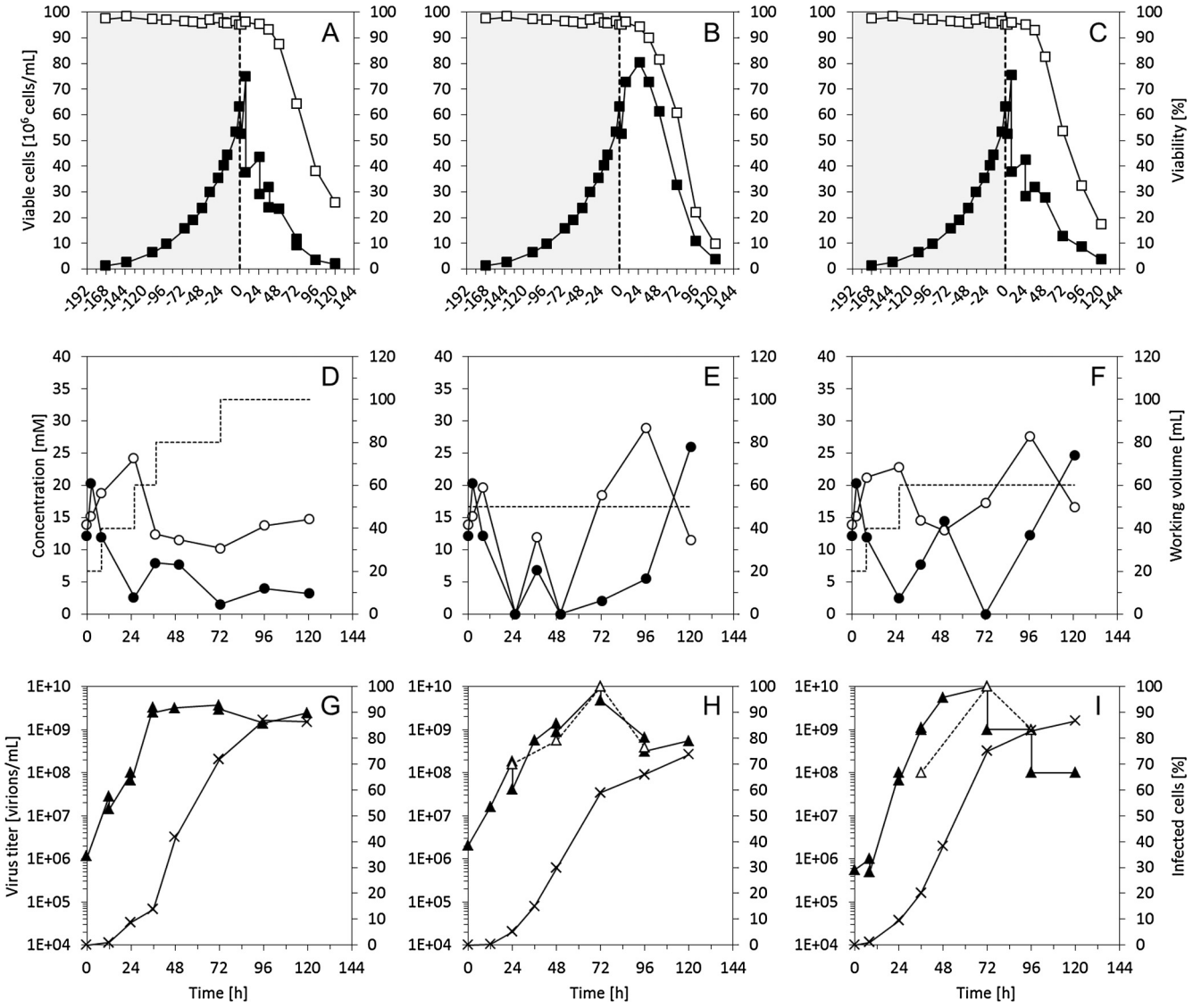


**Fig. 5.** MVA-CR19 virus production in CR.pIX cell using different feeding strategies. Fed-batch (FB) (A, D, G), daily medium exchange (DME) (B, E, H), and a combination of FB and DME (F+D) (C, F, I). Viable cell concentrations (■) and viability (□) at cell growth phase (shaded area) and virus propagation phase (white area). Glucose (●) and lactate (○) concentrations, working volume (dashed line). Virus titer in bioreactor (lysate) (▲) and harvest (supernatant) (△), percentage of infected cells (×). Cell growth phase (shaded area), virus propagation phase (white area).

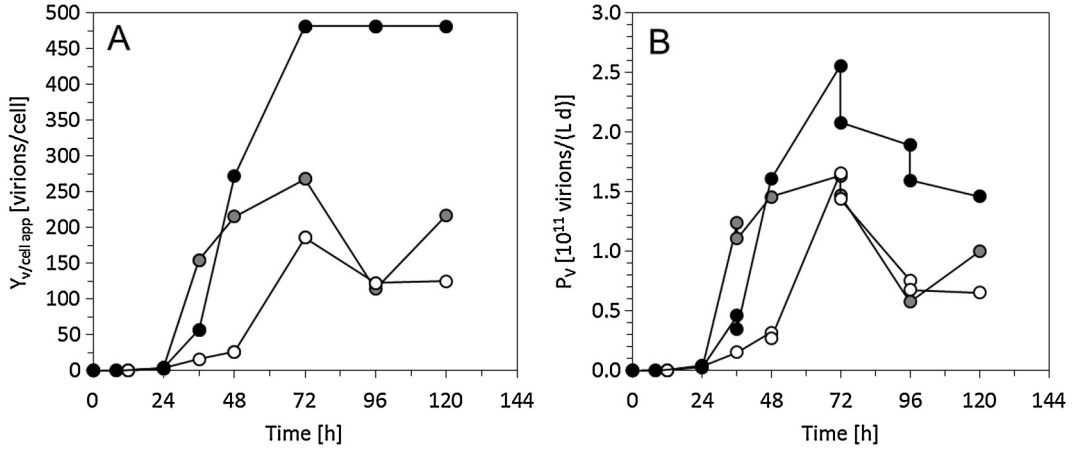


**Fig. 6.** Accumulated MVA-CR19 virus along the virus propagation phase. Apparent cell-specific yield ($Y_{v/cell\ app}$) (A) and volumetric productivity ($P_V$) (B) for FB (●), DME (○) and F+D (●) strategies.

**Table 3**
MVA-CR19 production in CR.pIX suspension cells in shake flasks for different feeding strategies after seed virus addition.*

| Mode | Harvest vol.[a] [mL] | Harvest titer [virions/mL] | Max. cells [$\times 10^9$] | Pooled titer[b] [virions/mL] | $Y_{v/cell}$ [virions/cell] | $P_V$ [virions/(L × d)] |
|---|---|---|---|---|---|---|
| FB | 100 | $3.7 \times 10^9$ | 1.9 | $3.7 \times 10^9$ | $2.0 \times 10^2$ | $1.6 \times 10^{11}$ |
| DME | H1: 45<br>H2: 45<br>H3: 50 | $1.6 \times 10^8$<br>$5.6 \times 10^8$<br>$1.0 \times 10^{10}$ | 4.0 | $3.8 \times 10^9$ | $1.3 \times 10^2$ | $1.7 \times 10^{11}$ |
| F+D | H1: 45<br>H2: 50 | $1.0 \times 10^8$<br>$1.0 \times 10^{10}$ | 1.9 | $5.3 \times 10^9$ | $2.7 \times 10^2$ | $2.6 \times 10^{11}$ |

* All data correspond to values obtained at/up to 72 hpi (time of highest virus titer and productivity yields).
[a] H: harvest.
[b] Titer of accumulated harvests.

For an implementation of both the DME and the F+D strategies in large-scale vaccine manufacturing, several limitations have to taken into account. For example, at production scale medium exchanges and product harvests cannot be done as fast as in scale-down systems. Accordingly, the use of ATF or other hollow fiber systems with an adequate membrane cut-off should be considered. Based on the results obtained here, adaptation and optimization of such culture formats should focus not only on an adequate substrate supply of cells immediately before and after infection but also on an optimal dilution of possible inhibitors of infection and appropriate virus harvest intervals.

## 4. Conclusion

High-cell-density (HCD) cultivations of CR.pIX cells in a bioreactor using an ATF-based perfusion system resulted in similar specific cell growth rates to those previously reported for the same cell line in conventional-cell-density (CCD) culture [30], and the parental cell line CR [22]. Optimum cell proliferation was obtained by a stoichiometric determination of perfusion rates based on the specific cell growth rate. With an optimal supply of nutrients during the exponential phase, an average specific growth rate of 0.019 $h^{-1}$ was achieved with a minimum of medium consumption. In combination with a complete medium exchange prior to infection, cell concentrations in 125 mL shake flasks (50 mL $V_w$) increased even further (up to 83 $\times$ $10^6$ cells/mL), and virus infection of cell populations exceeding $10^8$ cells/mL seem feasible.

A scale-down to shake flasks to optimize HCD cultivations demonstrated the capacity of CR.pIX cells to achieve specific growth rates of 0.023 $h^{-1}$ ($t_2$ = 30 h). Future scale-up studies may achieve an increased cell proliferation if parameters of shake flask cultivation are approximated in bioreactors. Such parameters may include an unregulated pH profile during the batch cultivation phase, in which pH decreases as lactate accumulates, and the indirect pH regulation with the exchange of medium during the perfusion phase. Dissolved oxygen and/or stirring speed may also have been underestimated and perhaps should be adjusted to avoid DO gradients.

The analysis of the scale-down model (shake flasks) suggested that maximum virus yields depend on a high viability of cells at TOI, and can be increased if conditioned medium is replaced at that time point. A partial medium replacement may dilute inhibitory metabolites and replenish nutrients that have been depleted during the cell proliferation phase. One process design that takes these observations into account employs a complete medium exchange, followed by fed-batch intervals. Such a strategy is a good option especially for viruses with replication cycles that are longer than the time needed to deplete the available glucose given in the initial medium exchange. Once this first critical stage is overcome, a (semi-) continuous medium exchange could be applied to collect infectious virus material and to avoid the accumulation of toxic by-products. A combination of all options allowed to increase the cell-specific virus yields compared to CCD cultivations and to achieve a very high volumetric productivity at HCD.

Overall, this study demonstrates that replication of MVA is not inhibited by high host cell density, and presents a general method which can be employed for maximizing yields of cell culture-derived vaccine viruses. Using existing bioreactors coupled to perfusion systems, HCD cultivations have the potential to outperform conventional production strategies, when implementing additional optimizations focusing on the challenges for scale-up discussed above. Consequently, the here studied culture formats may also allow (semi-)continuous cell-free virus harvesting and thus simplify the subsequent downstream processing.

## Acknowledgements

Daniel Vázquez-Ramírez would like to thank the Mexican National Council of Science and Technology (CONACyT) and the German Academic Exchange Service (DAAD) for their financial support to this project.

## Conflict of interest

The authors declare that they have no conflicts of interest.

## References

[1] Altenburg AF, Kreijtz JHCM, de Vries RD, Song F, Fux R, Rimmelzwaan GF, et al. Modified Vaccinia Virus Ankara (MVA) as production platform for vaccines against influenza and other viral respiratory diseases. Viruses-Basel 2014;6:2735–61.
[2] Mayr A, Munz E. Changes in the vaccinia virus through continuing passages in chick embryo fibroblast cultures. Zentralbl Bakteriol Orig 1964;195:24–35.
[3] Rimmelzwaan GF, Kreijtz JHCM, Suezer Y, Schwantes A, Osterhaus ADME, Sutter G. Preclinical evaluation of influenza vaccines based on replication-deficient poxvirus vector MVA. Procedia Vaccinol 2011;4.
[4] Ramezanpour B, Pronker ES, Kreijtz JHCM, Osterhaus ADME, Claassen E. Market implementation of the MVA platform for pre-pandemic and pandemic influenza vaccines: a quantitative key opinion leader analysis. Vaccine 2015;33:4349–58.
[5] Volz A, Sutter G. Protective efficacy of Modified Vaccinia virus Ankara in preclinical studies. Vaccine 2013;31:4235–40.
[6] Gomez CE, Perdiguero B, Garcia-Arriaza J, Esteban M. Clinical applications of attenuated MVA poxvirus strain. Expert Rev Vaccines 2013;12:1395–416.
[7] Gilbert SC. Clinical development of Modified Vaccinia virus Ankara vaccines. Vaccine 2013;31:4241–6.
[8] Hess RD, Weber F, Watson K, Schmitt S. Regulatory, biosafety and safety challenges for novel cells as substrates for human vaccines. Vaccine 2012;30:2715–27.
[9] Gomez CE, Perdiguero B, Garcia-Arriaza J, Esteban M. Poxvirus vectors as HIV/AIDS vaccines in humans. Hum Vacc Immunother 2012;8:1192–207.
[10] Boukhebza H, Bellon N, Limacher JM, Inchauspe G. Therapeutic vaccination to treat chronic infectious diseases: current clinical developments using MVA-based vaccines. Hum Vaccin Immunother 2012;8:1746–57.
[11] Gomez CE, Najera JL, Krupa M, Perdiguero B, Esteban M. MVA and NYVAC as vaccines against emergent infectious diseases and cancer. Curr Gene Ther 2011;11:189–217.
[12] Jordan I, Vos A, Beilfuss S, Neubert A, Breul S, Sandig V. An avian cell line designed for production of highly attenuated viruses. Vaccine 2009;27:748–56.

[13] Jordan I, Northoff S, Thiele M, Hartmann S, Horn D, Howing K, et al. A chemically defined production process for highly attenuated poxviruses. Biologicals 2011;39:50–8.
[14] Jordan I, Sandig V. Highly efficient, chemically defined and fully scalable biphasic production of vaccine viruses. BMC Proc 2011;5(Suppl 8):O1.
[15] Lohr V, Rath A, Genzel Y, Jordan I, Sandig V, Reichl U. New avian suspension cell lines provide production of influenza virus and MVA in serum-free media: studies on growth, metabolism and virus propagation. Vaccine 2009;27:4975–82.
[16] Jordan I, Horn D, John K, Sandig V. A genotype of Modified Vaccinia Ankara (MVA) that facilitates replication in suspension cultures in chemically defined medium. Viruses-Basel 2013;5:321–39.
[17] Tapia F, Vazquez-Ramirez D, Genzel Y, Reichl U. Bioreactors for high cell density and continuous multi-stage cultivations: options for process intensification in cell culture-based viral vaccine production. Appl Microbiol Biotechnol 2016.
[18] Henry O, Dormond E, Perrier M, Kamen A. Insights into adenoviral vector production kinetics in acoustic filter-based perfusion cultures. Biotechnol Bioeng 2004;86:765–74.
[19] Nadeau I, Kamen A. Production of adenovirus vector for gene therapy. Biotechnol Adv 2003;20:475–89.
[20] Lindsay DA, Betenbaugh MJ. Quantification of cell-culture factors affecting recombinant protein yields in baculovirus-infected insect cells. Biotechnol Bioeng 1992;39:614–8.
[21] Maranga L, Brazao TF, Carrondo MJT. Virus-like particle production at low multiplicities of infection with the baculovirus insect cell system. Biotechnol Bioeng 2003;84:245–53.
[22] Genzel Y, Vogel T, Buck J, Behrendt I, Ramirez DV, Schiedner G, et al. High cell density cultivations by alternating tangential flow (ATF) perfusion for influenza A virus production using suspension cells. Vaccine 2014;32:2770–81.
[23] Yuk IHY, Olsen MM, Geyer S, Forestell SP. Perfusion cultures of human tumor cells: a scalable production platform for oncolytic adenoviral vectors. Biotechnol Bioeng 2004;86:637–42.
[24] Van HH, Luitjens A. Method for the production of ad26 adenoviral vectors. Google Patents; 2011.
[25] Tapia F, Vogel T, Genzel Y, Behrendt I, Hirschel M, Gangemi JD, et al. Production of high-titer human influenza A virus with adherent and suspension MDCK cells cultured in a single-use hollow fiber bioreactor. Vaccine 2014;32:1003–11.
[26] Ghani K, Garnier A, Coelho H, Transfiguracion J, Trudel P, Kamen A. Retroviral vector production using suspension-adapted 293GPG cells in a 3L acoustic filter-based perfusion bioreactor. Biotechnol Bioeng 2006;95:653–60.
[27] Ozturk SS. Engineering challenges in high density cell culture systems. Cytotechnology 1996;22:3–16.
[28] Kompala DS, Ozturk SS. Optimization of high cell density perfusion bioreactors. In: Ozturk SS, Hu WS, editors. Cell culture technology for pharmaceutical and cell-based therapies. Boca Raton, FL: CRC Press, Taylor & Francis Group; 2006. p. 387–416.
[29] Lohr V, Hadicke O, Genzel Y, Jordan I, Buntemeyer H, Klamt S, et al. The avian cell line AGE1.CR.pIX characterized by metabolic flux analysis. Bmc Biotechnol 2014;14:72.
[30] Lohr V. Characterization of the avian designer cells AGE1.CR and AGE1.CR.pIX considering growth, metabolism and production of influenza virus and Modified Vaccinia Virus Ankara (MVA). Magdeburg, Germany: Otto von Guericke University Magdeburg; 2014.
[31] Lohr V, Genzel Y, Jordan I, Katinger D, Mahr S, Sandig V, et al. Live attenuated influenza viruses produced in a suspension process with avian AGE1.CR.pIX cells. Bmc Biotechnol 2012;12.
[32] Schiefelbein S, Frohlich A, John GT, Beutler F, Wittmann C, Becker J. Oxygen supply in disposable shake-flasks: prediction of oxygen transfer rate, oxygen saturation and maximum cell concentration during aerobic growth. Biotechnol Lett 2013;35:1223–30.
[33] Pohlscheidt M, Langer U, Minuth T, Bodeker B, Apeler H, Horlein HD, et al. Development and optimisation of a procedure for the production of *Parapoxvirus ovis* by large-scale microcarrier cell culture in a non-animal, non-human and non-plant-derived medium. Vaccine 2008;26:1552–65.